An efficient deep learning approach for predicting the ultimate load and maximum lateral web deformation of unstiffened steel plate girders under patch loading

Dai-Nhan Le[1] Quang-Viet Vu[2] and Sawekchai Tangaramvong[1]

[1] *Center of Excellence in Applied Mechanics and Structures, Department of Civil Engineering, Chulalongkorn University, Bangkok 10330, THAILAND*

[2] *Faculty of Advanced Technology and Engineering, VNU Vietnam Japan University, Hanoi, 100000, VIETNAM*

**Corresponding author; E-mail address: sawekchai.t@chula.ac.th*

Abstract

The maximum web deformation, along with the ultimate load, plays a crucial role in estimating the behavior of unstiffened steel plate girders subjected to patch loading. While various machine learning (ML) approaches have been applied to predict the ultimate load of the girders based on experimental or numerical datasets, no research has been conducted to predict both the ultimate load and the maximum lateral web deformation simultaneously. Therefore, this study introduces an efficient method for predicting both factors using a multi-layer perceptron (MLP) model. Initially, a Python-based program was developed to create a finite element (FE) model of unstiffened steel plate girders under patch loading, validated against experimental data. This validated model was used to generate a dataset of 500 FE simulations with various girder geometries and material strengths. Subsequently, this dataset was employed to train an MLP model. The Differentiable Architecture Search (DARTS) method is then applied to optimize the MLP architecture to enhance the performance of the MLP model. The proposed DARTS-MLP model demonstrated high accuracy in predicting the ultimate load and maximum lateral web deformation, closely matching the true values in the test set. The DARTS-MLP's predictions were compared with existing design codes and empirical formulae, further confirming its prediction accuracy. Finally, a web-based application was developed to apply the proposed DART-MLP model in practical design.

Keywords: Deep learning, Finite Element Method, Differentiable Architecture Search, unstiffened steel plate girder.

1. Introduction

Patch loading refers to the application of concentrated loads over a small area on the structural component. This type of loading is critical in structural engineering, especially in bridge construction, where girders are often subjected to localized forces during launching or in service [1]. In practical design, Steel plate girders (SPG) are highly effective in resisting patch loading due to their structural efficiency, high load-bearing capacity, and adaptability [2]. Their excellent strength-to-weight ratio allows them to carry concentrated loads without excessive deformation, while the combination of a wide flange and a deep web helps distribute patch loads efficiently, reducing localized stress concentrations. The flexibility in design enables engineers to optimize web thickness, flange size, and stiffener configurations to enhance resistance against local buckling. Additionally, the incorporation of longitudinal and transverse stiffeners significantly improves load resistance, increasing the girder's ultimate capacity. While SPG offers numerous advantages for patch loading, its behavior is complex and involves interactions between material properties, geometric parameters, boundary conditions, and so on. Under certain conditions, such as when the web depth exceeds 150 times the thickness of the web plate, an unstiffened girder may be used instead of a stiffened girder, according to the AASHTO LRFD standard [3]. Fig. 1 shows an unstiffened SPG subjected to patch loading. In this diagram, (h_w, t_w) represents the dimensions of the web plates, while (b_f, t_f) indicates the dimensions of the flange plates. Additionally, a denotes the length of the girder, and Ss represents the length of the applied load area.

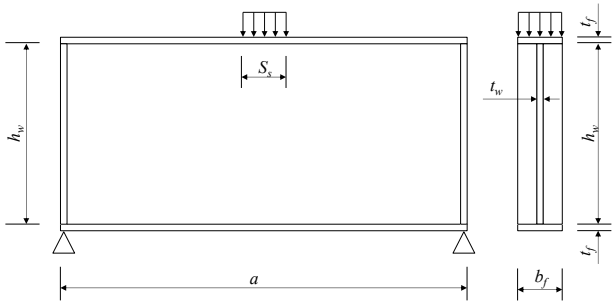

Fig. 1 The unstiffened SPG under patch loading.

In structural design, it is insufficient to consider only the ultimate load of the SPG under patch loading for a complete assessment. The deformation of the web panel plays a crucial role as it is related to the stability of the girder. Therefore, it is important to consider both the ultimate load and the

corresponding web deformation of unstiffened panels subjected to patch loading [4]. Traditional approaches for this assessment include conducting experiments or using finite element analysis (FEA) [5]. Recently, Kovacevic and Markovic investigated the effect of patch load length on the behaviors of SPGs [6]. In these experiments, the deformation of the web plate was also estimated. Using the FEA approach, Luo et al. [7] considered the patch loading resistance of high-strength steel plate girders by using a numerical modelling method validated by 39 experimental results to analyze the effects of various parameters, including web aspect ratios and height-to-thickness ratios, on ultimate resistance.

While traditional methods can produce reliable results, they are difficult to implement in practical design due to high resource demands and the need for specialized expertise. Therefore, the machine learning (ML) approach is increasingly applied in the field of structural design for its many advantages, including the ability to analyze complex relationships between variables, optimize design parameters efficiently, and improve predictive accuracy [8]. As a result, numerous ML models have been deployed on unstiffened SPG under patch loading. Recently, Kong et al. [9] proposed a hybrid machine learning with optimization algorithm and resampling methods to predict the patch loading resistance of both longitudinally unstiffened and stiffened plate girders, based on experimental data collected from the literature. This model was compared with seven other hybrid models and achieved the best accuracy in term of various metrics. The results showed that the resampling method effectively reduces the gap between training and testing sets, improving the prediction reliability with limited data. Le et al. [10] also developed hybrid ML models to estimate the ultimate load of unstiffened SPGs under patch loading. Among the five evaluated models, BO-GBT demonstrated the highest accuracy in predicting the ultimate load. In addition, the predictive results obtained from the proposed model were shown to surpass the performance of design standards and empirical formulas, confirming the reliability and accuracy of the proposed model within the studied data range. However, most of these models primarily focus on predicting the ultimate load or failure modes [11], with limited attention given to estimating web deformation. Additionally, the databases used for training the ML models in existing research were mainly collected from experiments that were limited, leading to a narrow range of application in practical design.

To address this gap, this study develops a multi-layer perceptron (MLP) model for predicting both the ultimate load and the maximum web deformation. A Python-based program is developed to generate a finite element (FE) model of unstiffened SPG under patch loading, which is validated against experimental data. The validated model is then used to create a dataset of 500 FE simulations covering various girder geometries and material properties for training the MLP model. To optimize the MLP architecture, the Differentiable Architecture Search (DARTS) method is applied. The performance of the proposed DARTS-MLP model is demonstrated through the evaluation metrics of the predictive results on the test set. Additionally, the accuracy and reliability of the proposed model are compared with existing design codes and empirical formulas. Finally, the web-based application is created to deploy the proposed model without requiring ML knowledge and programing skills.

2. Finite element modeling

2.1 FE modelling of unstiffened SPG

The ABAQUS software is employed to simulate an unstiffened SPG under patch loading. A 3D finite element (FE) model is developed using Python script. S4R shell elements are used to model all girder components with a mesh size of 25 mm × 25 mm. The constitutive material models of girder components are taken from tensile test results of the material reported in [12]. For models without test results of the constitutive material model, a tri-linear stress-strain relationship of the material properties is employed as suggested in [12]. In the FE model, the flanges, web, and end plates are connected using the *TIE CONSTRAINT option to prevent relative movement. A reference point (RP1) and rigid body constraint are defined in the top flange of the SPG to ensure the load transfer. Boundary conditions include hinge and roller supports, with horizontal movement restrained. Initial geometric imperfections, which are derived from buckling analysis, are introduced using the *IMPERFECTION option, with magnitudes of $h_w/100$ or $h_w/200$, aligning with the EC3 design code [13]. The final results are obtained from the Post-buckling analysis using the RIKS algorithm. The FE model of the unstiffened SPG is shown in Fig. 2.

2.2 Verification of the FE model

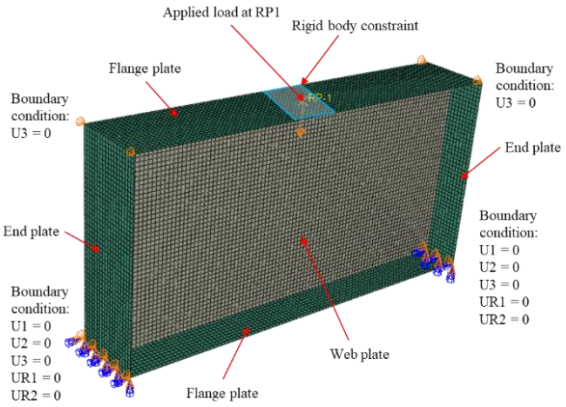

Fig. 2 The FE model of unstiffened SPG under patch loading.

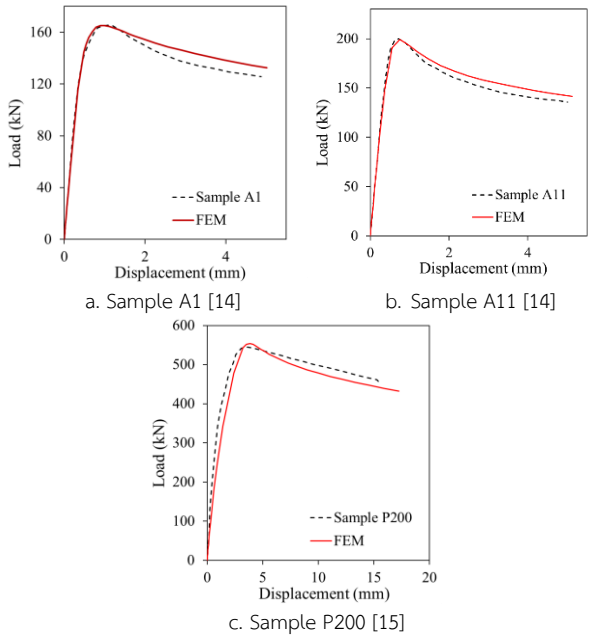

a. Sample A1 [14] b. Sample A11 [14]

c. Sample P200 [15]

Fig. 3 The comparisons between FEM and results in the experiments of Kovacevic et al. [14] and Gozzi [15].

To validate the accuracy of the FE model, the load-displacement curves obtained from these FE models are compared with those from three experimental tests reported by Kovacevic et al [14] and Gozzi [15]. The comparisons provided in Fig. 3 present a good agreement between the FE and the experimental results for all girders. This indicates that the FE model is capable of capturingthe behavior of unstiffened SPG subjected patch loading. These findings demonstrate that the developed FE model can serve as a robust tool for analyzing structural behavior and generating the FE dataset for ML models.

3. Dataset generation

Table 1 The statistical value of parameters.

Parameters	Min	Max	Mean	STD
b_f (mm)	100.00	330.00	201.14	63.69
t_f (mm)	5.00	20.00	14.55	3.34
h_w (mm)	570.00	2000.00	1204.74	382.53
t_w (mm)	4.00	14.00	9.46	3.15
a (mm)	630.00	5510.00	2403.40	1089.43
S_s (mm)	120.00	2470.00	724.20	450.47
f_{yf} (MPa)	290.00	450.00	373.21	55.01
f_{uf} (MPa)	415.00	550.00	481.51	47.59
f_{yw} (MPa)	290.00	450.00	377.29	56.36
f_{uw} (MPa)	415.00	550.00	485.29	48.94
P_u (kN)	190.70	2989.32	1115.08	552.54
d_u (mm)	4.52	80.75	28.33	14.84

Based on the developed FE model, a dataset consisting of 500 samples is generated for training the ML model. The input parameters consist of the geometry of the unstiffened SPG shown in Fig. 1, along with the yield and ultimate strengths of the web (f_{yw}, f_{uw}) and the flange (f_{yf}, f_{uf}) plates. The output variables are the ultimate load (P_u) and the corresponding lateral web deformation (d_u). The statistical values of each parameter are shown in Table 1. As can be seen from Table 1, the parameters exhibit considerable variability. For example, the height of the web panel (h_w) ranges from 570 mm to 2000 mm, with a standard deviation (STD) of 382.53 mm. This variability provides the machine learning (ML) model with a diverse range of values, enhancing its ability to generalize and improve accuracy in various scenarios. Therefore, using this FE dataset, ML models can achieve a high-accuracy prediction when predicting the ultimate load and web deformation of the unstiffened SPG.

4. Methodology

4.1 Multilayer Perceptron (MLP)

A Multilayer Perceptron (MLP) [15] is a type of artificial neural network that consists of several layers of neurons, including an input layer, one or more hidden layers, and an output layer. Each neuron in a given layer is connected to every neuron in the following layer, creating a fully connected network. The MLP processes input data by applying a series of weighted transformations, followed by activation functions. This can allow the network to learn complex patterns and relationships within the data. The output of a neuron in a hidden layer is calculated by:

$$z^{(i)} = W^{(i)} x^{(i-1)} + b^{(i)} \quad (1)$$

Where $z^{(i)}$, $W^{(i)}$, and $b^{(i)}$ are the weighted sum of inputs, weight matrix, and bias term of the layer i, respectively. $x^{(i-1)}$ is the output of the previous layer. To capture the nonlinear relationships between the input and output variables. The final output of each neuron in layer i is computed with the activation function:

$$x^{(i-1)} = \sigma\left(z^{(i)}\right) \quad (2)$$

Where $\sigma(.)$ is the activation function, such as ReLU, Sigmoid, or Tanh [16]. The typical MLP model with two inputs, one output variable and two hidden layers with three neurons in each layers is presented in Fig. 4.

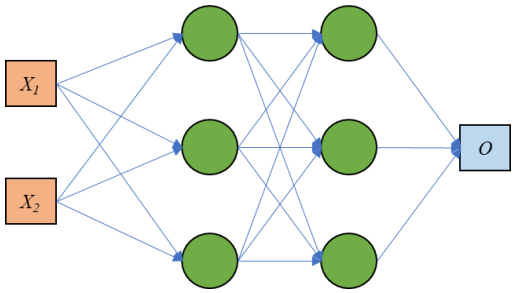

Fig. 4 The typical MLP model.

4.2 Differentiable Architecture Search (DARTS)

Differentiable Architecture Search (DARTS) [17] is a powerful neural architecture search (NAS) method that is used to find optimal deep learning architectures by making the search process differentiable. Unlike traditional NAS techniques, which rely on computationally expensive reinforcement learning or evolutionary algorithms, DARTS formulates the architecture search as a continuous optimization problem, allowing gradient-based methods to be used for efficient optimization. The DART method consists of two main concepts, including Search space representation and Continuous relaxation and optimization.

4.2.1 Search space representation

In DARTS, the neural network architecture is modelled as a directed acyclic graph (DAG), where nodes correspond to feature maps (activations) at different layers, and edges represent candidate operations such as convolutions, pooling, or identity mapping that transform these feature maps. Rather than selecting a single discrete operation for each edge, DARTS assigns a weighted sum of all possible operations, allowing the architecture search process to be continuously relaxed. This continuous formulation makes the search differentiable, enabling efficient optimization using gradient-based methods.

4.2.2 Continuous relaxation and optimization

While traditional NAS methods require a discrete selection of operations, DARTS replaces discrete choices with a softmax-weighted sum of all candidate operations, allowing gradient-based optimization:

$$\bar{o}^{(i,j)}(x) = \sum_{o \in O} \frac{\exp\left(\alpha_o^{(i,j)}\right)}{\sum_{o' \in O} \exp\left(\alpha_{o'}^{(i,j)}\right)} \times o(x) \tag{3}$$

Where $\alpha_o^{(i,j)}$ is the learnable weight associated with operation o on edge (i,j).

The network weights w and architecture parameters α through a bi-level optimization problem. In this process, the inner optimization finds the optimal weights $w^*(\alpha)$ for a given architecture α, while the outer optimization updates α to minimize validation loss. The equation can be presented as:

$$\min_{\alpha} L_{val}\left(w^*(\alpha), \alpha\right)$$
$$\text{Subject to } w^*(\alpha) = \arg\min_{\alpha} L_{train}\left(w, \alpha\right) \tag{4}$$

Where $\mathcal{L}_{val}$ and $\mathcal{L}_{train}$ are validation and training losses, respectively.

In this study, the network weights and architecture parameters are optimized with Adam optimizer.

5. The proposed DARTS-MLP model

The procedure for developing the proposed DARTS-MLP model to predict the ultimate load and maximum web deformation of the unstiffened under patch loading is described in the following steps.

Step 1: Data dividing and normalizing

To train the proposed model, the dataset is divided into the training, validation, and test sets with a 70-15-15 ratio. Moreover, all features in this dataset are normalized in the range [0, 1] for better convergence and to ensure that all features contribute equally to the learning process.

Step 2: Define the training process

To obtain the optimal model, the Adam optimizer is used to optimize both the architecture and the weights of the MLP model. The architecture of the MLP model is described with the number of hidden layers (n_layers), the number of neurons in each layer (n_neurons_i), and the activation function in each layer (activation_i). The learning rate is set to 0.001, and the loss function to be minimized is the Mean Squared Error (MSE). The illustration of MLP's architecture and the search space are shown in Fig. 5 and Table 2.

Table 2 The search space of the DARTS.

Hyperparameters	Range
n_layers	[1, 5]
n_neurons_i	[32, 128]
activation_i	[relu, tanh, sigmoid]

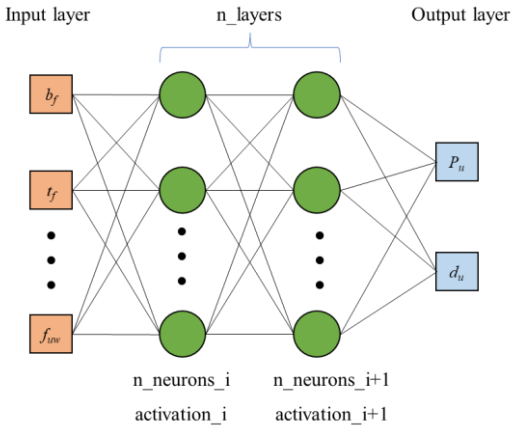

Fig. 5 The architecture of MLP model.

Step 3: Train the proposed model

The training procedure with 1000 epochs is shown in Fig. 6. The MLP model is updated according to the training set accuracy, while the optimal model being the one that achieves the highest accuracy on the validation set.

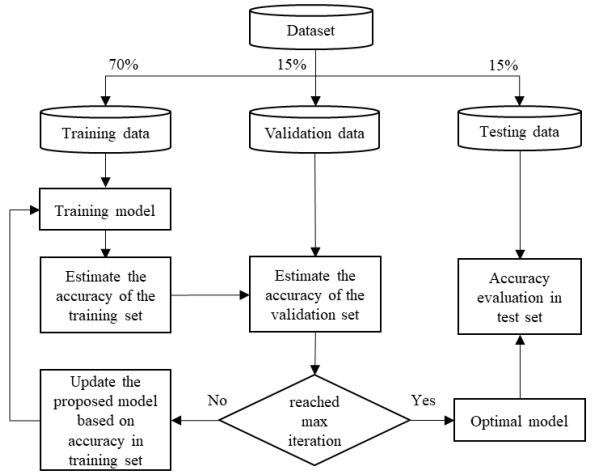

Fig. 6 The training procedure of the proposed model.

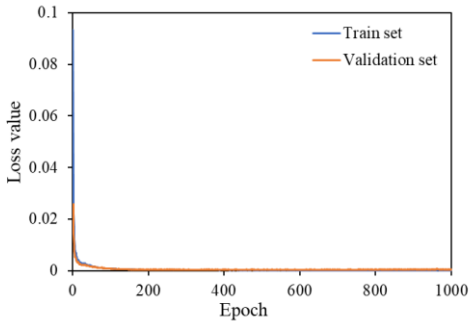

Fig. 7 The optimization result of the proposed model.

The optimization result is presented in Fig. 7. It can be seen that the values of the loss function for both the training and validation sets converge after 200 epochs, approaching zero. This indicates that the DARTS method successfully identifies the optimal architecture for the MLP model in this study. Furthermore, the optimal architecture can be determined in earlier epochs. The architecture of the proposed DARTS-MLP model is described in Table 3.

Table 3 The architecture of the proposed DARTS-MLP model.

Hyperparameters	Range
n_layers	2
n_neurons_1	54
activation_1	Tanh
n_neurons_2	77
activation_i	ReLU

6. Performance proposed DARTS-MLP model

6.1 Metric evaluation

In this study, the accuracy of the proposed model's predictions is evaluated with four popular metrics, including R-squared (R^2), Root Mean Square Error (RMSE), Mean Absolute Error (MAE), and A20-index [10]. The evaluated value of each metric is presented in Table 4.

It can be seen that the model achieves an impressive coefficient of determination (R^2 = 0.99) for the ultimate load across all three sets. This indicates that the model effectively captures the relationship between the input parameters and the target variables. The RMSE values are 37.0 kN for the training set, 60.3 kN for the validation set, and 57.4 kN for the test set. Additionally, the MAE values are 26.6 kN, 45.8 kN, and 42.0 kN for the respective sets, which demonstrates that the average deviation between predicted and actual values is relatively low. Furthermore, the A20-index scores are nearly perfect, with a value of 1.0 for both the training and validation sets, and 0.99 for the test set. This indicates that most predictions fall within an acceptable error range of ±20% of the actual values.

Table 4 The architecture of the proposed DARTS-MLP model.

Output variable	Dataset	Metric			
		R^2	RMSE	MAE	A20-index
Ultimate load	Training set	0.99	37.0 (kN)	26.6 (kN)	1.0
	Validation set	0.99	60.3 (kN)	45.8 (kN)	1.0
	Test set	0.99	57.4 (kN)	42.0 (kN)	0.99
Maximum lateral web deformation	Training set	0.99	1.19 (mm)	0.92 (mm)	0.98
	Validation set	0.98	1.97 (mm)	1.48 (mm)	0.96
	Test set	0.98	2.24 (mm)	1.71 (mm)	0.95

Similarly, the proposed model demonstrates exceptional performance in predicting maximum lateral web deformation, achieving an R^2 value of 0.98 across all datasets. The RMSE values are 1.19 mm for the training set, 1.97 mm for the validation set, and 2.24 mm for the test set. Additionally, the MAE values are 0.92 mm, 1.48 mm, and 1.71 mm for the training, validation, and test sets, respectively. Furthermore, the A20-index values are 0.98 for the training set, 0.96 for the validation set, and 0.95 for the test set. The prediction accuracies validate the model's reliability and its strong generalization capabilities on previously unseen data.

6.2 Comparisons with existing formulae

In this section, the predictions of the proposed DARTS-MLP model are compared with the existing formulae proposed in previous studies and design code. These formulae are shown below.

The equation in the EC3 design code [13]:

$$P_u = \frac{f_{yw} \times L_{eff} \times t_w}{1.1} \quad (5)$$

Where:

$$L_{eff} = \chi_F \times l_y;\ \chi_F = \frac{0.5}{\bar{\lambda}_F} \le 1.0$$

$$l_y = S_s + 2t_f \times \left(1 + \sqrt{m_1 + m_2}\right) \le a;\ m_1 = \frac{f_{yf} \times b_f}{f_{yw} \times t_w}$$

$$\bar{\lambda}_F = \sqrt{\frac{F_y}{F_{cr}}};\ F_y = f_{yw} \times t_w \times l_y$$

$$m_2 = \begin{cases} 0.02 \times \left(\frac{h_w}{t_f}\right)^2 & if\ \bar{\lambda}_F > 0.5 \\ 0 & if\ \bar{\lambda}_F \le 0.5 \end{cases}$$

The proposed formula of Skaloud et al [18] :

$$P_u = 0.55 \times t_w (0.9 \times t_w + 1.5 \times S_s \times t_w / h_w) \sqrt{E \times f_{yw}} \times \sqrt{t_f / t_w} \quad (6)$$

The proposed formula in Drdacky's study [19]:

$$P_u = 19.54 \times t_w^2 \times f_{yw} \times (1 + 0.0004 \times S_s / t_w)(I_f / t_w^4)^{0.1} \quad (7)$$

The equation proposed by Roberts and Newark [20]:

$$P_u = \left(1.1 \times t_w^2 \times \sqrt{E \times f_{yw}} \times \left(t_f / t_w\right)^{1/4} \times \left(1 + \frac{S_{se} \times t_w}{h_w \times t_f}\right)\right) / F \quad (8)$$

$$F = 1.45;\ S_{se} = S_s + 2 \times t_f$$

The comparisons between the proposed DARTS-MLP model and existing design formulae in all three sets are presented in Figs.8-10. It can be observed that the ratio between the prediction and FEM results of the existing equations ranges from 0.4 to 2.3. In contrast, the ratios for the proposed DARTS-MLP model are more consistent, clustering between 0.9 and 1. The DARTS-MLP model shows a significant improvement in prediction accuracy compared to existing design equations. The narrower range of the estimated ratios indicates that this model effectively captures the underlying structural behavior of unstiffened SPG under patch loading. Additionally, the reduced variation in prediction errors suggests that the proposed model can provide more reliable and practical estimations for engineering applications.

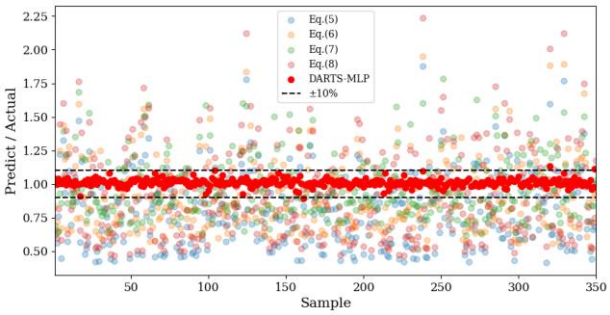

Fig. 8 The comparison between the proposed DARTS-MLP model and existing design formulae in the training set.

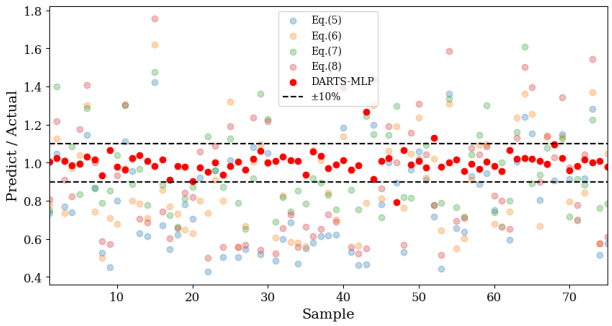

Fig. 9 The comparison between the proposed DARTS-MLP model and existing design formulae in the validation set.

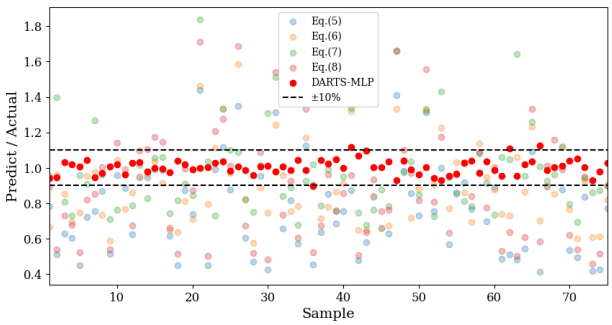

Fig. 10 The comparison between the proposed DARTS-MLP model and existing design formulae in the test set.

7. Web-based application

In this section, the proposed DART-MLP model is implemented as a user-friendly Graphical User Interface (GUI) on the Hugging Face platform. The tool enables users to predict the ultimate load and its corresponding web lateral deformation of the unstiffened SPGs under patch loading based on input variables, without requiring prior knowledge of simulation or machine learning. This tool can reduce simulation time and experimental costs by allowing users to explore expected outcomes in advance. The developed application is illustrated in Fig. 11 and can be accessed via the following link: https://huggingface.co/spaces/DaiNhanLe/DART-MLP.

Fig. 11 The comparison between the proposed DARTS-MLP model and existing design formulae in the training set.

8. Conclusions

An efficient deep learning approach for predicting the ultimate load and maximum lateral web deformation of unstiffened steel plate girder under patch loading is introduced in this study. The MLP model is trained using a FE dataset, which is created through numerical analysis. The DARTS method is applied to determine the optimal architecture for the MLP model. Based on the observed results of the proposed method, it can be concluded that the FE model produces outputs closer to experimental results, making it suitable for generating data to train machine learning models. The DARTS method significantly impacts the optimization of the MLP's architecture. Furthermore, the prediction results indicate that the proposed DARTS-MLP model demonstrates strong performance when evaluated using various metrics and compared to existing formulas. These results, along with the developed web application, present a powerful approach for structural engineers that not only improves predictive accuracy but also provides a data-driven alternative to traditional design formulas, potentially leading to more efficient and optimized structural designs.

Acknowledgement

The authors gratefully acknowledge the support provided by the Graduate Scholarship Program for ASEAN or Non-ASEAN Countries, Chulalongkorn University, awarded to Dai-Nhan Le.

References

[1] Tetougueni CD, Maiorana E, Zampieri P, Pellegrino C. Plate girders behaviour under in-plane loading: A review. Eng Fail Anal 2019;95:332–58. https://doi.org/10.1016/J.ENGFAILANAL.2018.09.021.

[2] Terreros-Bedoya A, Negrin I, Payá-Zaforteza I, Yepes V. Hybrid steel girders: Review, advantages and new horizons in research and applications. J Constr Steel Res 2023;207:107976. https://doi.org/10.1016/J.JCSR.2023.107976.

[3] American Association of State Highway and Transportation Officials. AASHTO LRFD standard. 2008.

[4] Chen XW, Yuan HX, Du XX, Zhu ZW. Nonlinear deformation behaviour and design of welded stainless steel I-section flexural members. Eng Struct 2022;252:113683. https://doi.org/10.1016/J.ENGSTRUCT.2021.113683.

[5] Chen B, Dai Y, Wang Y, Wang Y, Song Y, Luo L, et al. Patch-loading resistance of QN1803 and S32001 high-strength stainless steel plate girders: Experimental study and numerical simulation. Thin-Walled Structures 2025;206:112681. https://doi.org/10.1016/J.TWS.2024.112681.

[6] Kovacevic S, Markovic N. Experimental study on the influence of patch load length on steel plate girders. Thin-Walled Structures 2020;151:106733. https://doi.org/10.1016/J.TWS.2020.106733.

[7] Luo Z, Shi Y, Xue X, Li H, Xu J. High-strength steel plate girders under patch loading: Numerical analysis and design recommendations. Structures 2023;57:105108. https://doi.org/10.1016/J.ISTRUC.2023.105108.

[8] Nath D, Ankit, Neog DR, Gautam SS. Application of Machine Learning and Deep Learning in Finite Element Analysis: A Comprehensive Review. Archives of Computational Methods in Engineering 2024 31:5 2024;31:2945–84. https://doi.org/10.1007/S11831-024-10063-0.

[9] Kong Z, Le DN, Pham TH, Poologanathan K, Papazafeiropoulos G, Vu QV. Hybrid machine learning with optimization algorithm and resampling methods for patch load resistance prediction of unstiffened and stiffened plate girders. Expert Syst Appl 2024;249:123806. https://doi.org/10.1016/J.ESWA.2024.123806.

[10] Le DN, Pham TH, Papazafeiropoulos G, Kong Z, Tran VL, Vu QV. Hybrid machine learning with Bayesian optimization methods for prediction of patch load resistance of unstiffened plate girders. Probabilistic Engineering Mechanics 2024;76:103624. https://doi.org/10.1016/J.PROBENGMECH.2024.103624.

[11] Tran VL, Kim JK. Hybrid machine learning models for classifying failure modes of unstiffened steel plate girders subjected to patch loading. Structures 2024;59:105742. https://doi.org/10.1016/J.ISTRUC.2023.105742.

[12] Bonilla J, Mirambell E, Arrayago I. Numerical analysis of curved steel plate girders subjected to patch loading. Eng Struct 2023;297:117015. https://doi.org/10.1016/J.ENGSTRUCT.2023.117015.

[13] EN1993-1-5. Eurocode 3: Design of steel structures - Part 1-5: General rules - Plated structural elements 5. 2006.

[14] Kovacevic S, Markovic N, Sumarac D, Salatic R. Influence of patch load length on plate girders. Part II: Numerical research. J Constr Steel Res 2019;158:213–29. https://doi.org/10.1016/J.JCSR.2019.03.025.

[15] J. Gozzi, Patch loading resistance of plated girders: ultimate and serviceability limit state, Ph.D. thesis, Lulea tekniska universitet (2007).

[16] Chen Z, Li X, Wang W, Li Y, Shi L, Li Y. Residual strength prediction of corroded pipelines using multilayer perceptron and modified feedforward neural network. Reliab Eng Syst Saf 2023;231:108980. https://doi.org/10.1016/J.RESS.2022.108980.

[17] Dubey SR, Singh SK, Chaudhuri BB. Activation functions in deep learning: A comprehensive survey and benchmark. Neurocomputing 2022;503:92–108. https://doi.org/10.1016/J.NEUCOM.2022.06.111.

[18] Liu H, Simonyan K, Yang Y. DARTS: Differentiable Architecture Search. 7th International Conference on Learning Representations, ICLR 2019 2018.

[19] Skaloud M, Drdacky M. Ultimate load design of webs of steel plated structures-Part 3 Webs under concentrated loads. Staveb Casopis 1975;23:140–60.

[20] Drdacky M. Limit states of steel plate girder webs under patch loading. Proceedings, Regional Colloquium on Stability of Steel Structures, 1986, p. 687–94.

[21] Roberts TM, Newark ACB. Strength of webs subjected to compressive edge loading. Journal of Structural Engineering 1997;123:176–83.